

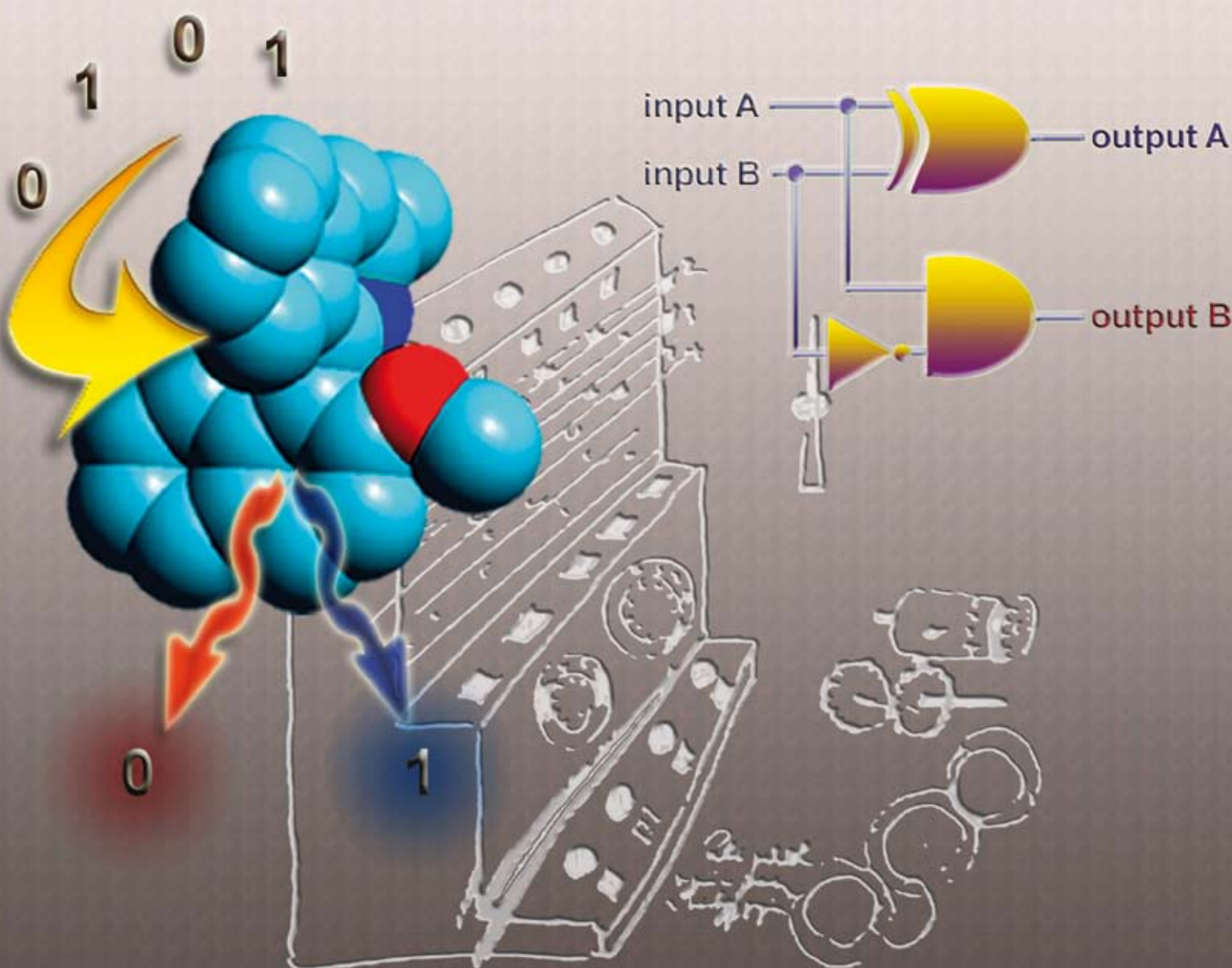
# NJC

New Journal of Chemistry

An international journal of the chemical sciences

www.rsc.org/njc

Volume 32 | Number 3 | March 2008 | Pages 369–556



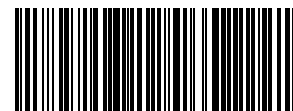
ISSN 1144-0546

RSC Publishing


 CENTRE NATIONAL  
DE LA RECHERCHE  
SCIENTIFIQUE

## PAPER

Uwe Pischel and Barbara Heller  
Molecular logic devices (half-subtractor,  
comparator, complementary output  
circuit) by controlling photoinduced  
charge transfer processes



1144-0546(2008)32:3;1-4

# Molecular logic devices (half-subtractor, comparator, complementary output circuit) by controlling photoinduced charge transfer processes

Uwe Pischel<sup>\*ab</sup> and Barbara Heller<sup>c</sup>

Received (in Montpellier, France) 4th July 2007, Accepted 29th August 2007

First published as an Advance Article on the web 10th September 2007

DOI: 10.1039/b710216j

The fluorescence properties of a naphthalene derivative with a methoxy and a pyridyl substituent were investigated, including the influence of protons, electron-donating amines, and dihydrogenphosphate anions. The naphthalene derivative shows strong fluorescence with a maximum at 353 nm, which can be quenched by amines through a diffusion-controlled photoinduced electron transfer. Protonation of the pyridyl residue leads to the observation of a red-shifted broad emission at 470 nm, which has been assigned to an internal charge transfer state. The interpretation of the fluorescence behaviour in the presence or absence of the chemical inputs leads to the realisation of unimolecular logic circuits, which are able to perform advanced arithmetic operations such as subtraction (*XOR/INH* combination) and comparison (*XNOR/INH* combination). Furthermore, a complementary output circuit (*INH/IMP* combination) was implemented. The implicated logic gates can be reconfigured, either by application of different input sets or by varying the fluorescence output observation wavelength. The system works in an all-fluorescence output mode, which leads to a superposition of the gates. This is of particular advantage as it allows reading out without any time lag, which is a commonly encountered problem in silicon circuitry based on electrical signals.

## Introduction

The realisation of logic functions with ion-, electro- or photo-switchable molecules is currently in the focus of research related to the increasing demands for further miniaturisation in information technology. Nowadays, all common essential logic gates, which are used in conventional silicon circuitry, can be mimicked at the molecular level with chemical or optical signals.<sup>1–5</sup> A step ahead is the small-scale integration of advanced functions such as adding, subtracting or comparing binary encoded inputs, which requires the combination of several logic gates.<sup>5</sup> One approach towards such devices is the parallel processing<sup>6</sup> of logic information by different chemical entities, which are operated by an identical set of inputs. The first molecular half-adder by de Silva *et al.* is based on such strategy and later other examples have been published.<sup>7,8</sup> However, the different molecular logic gates are required to work in a compatible manner, as interferences in form of chemical cross talk might lead to complications. The implementation of several gates with the same molecular entity by output-sided logic reconfiguration could be one approach to avoid these problems, albeit realistically seen, the number of available functions might be limited. Photoactive logic sys-

tems, which produce optical signals such as changes in the absorption or fluorescence spectrum, have attracted special attention, as the output can be potentially reconfigured by a simple change of the observation signal wavelength. Further, simultaneous monitoring of several absorption or fluorescence wavelengths leads to the superposition of logic gates,<sup>9,10</sup> which is inherently unknown to silicon-based analogues.<sup>3</sup>

In the present work we introduce the fluorescent pyridine-substituted naphthalene **1** (Scheme 1) as a very simple unimolecular system,<sup>†</sup> which unifies the concepts of reconfigurability and superposition in a multifaceted manner. We were able to control its logic response on the basis of intra- and intermolecular charge transfer processes by varying chemical input and optical output signals. This led to *XOR*, *XNOR*, *INH*, and *IMP* gates. Their combinations yield advanced logic devices such as a half-subtractor, a magnitude comparator, and a complementary output circuit.<sup>8,11–20</sup>

## Results and discussion

### Fluorescence properties of **1** and its protonated form **1H**<sup>+</sup>

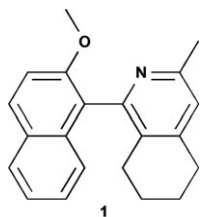
The absorption spectrum of **1** in acetonitrile solution consists of structured bands between 250 and 300 nm and above 300 nm. The first one has a maximum at 280 nm (molar absorption coefficient  $\epsilon = 8200 \text{ dm}^3 \text{ mol}^{-1} \text{ cm}^{-1}$ ) and the second band at 335 nm ( $\epsilon = 3300 \text{ dm}^3 \text{ mol}^{-1} \text{ cm}^{-1}$ ). This situation is typical for naphthalenes with donor substituents in 2-position, *e.g.*, methoxy,<sup>21</sup> which tend to lower the energy of  $\pi, \pi^*$ -excited

<sup>†</sup> The (*R*)-enantiomer of **1**, *i.e.*, (+)-(*R*)-1-(2-methoxynaphthalen-1-yl)-3-methyl-5,6,7,8-tetrahydroisoquinoline, was used.

<sup>a</sup> Departamento de Ingeniería Química, Química Física y Química Orgánica, Facultad de Ciencias Experimentales, Universidad de Huelva, Campus de El Carmen, E-21071 Huelva, Spain. E-mail: uwe.pischel@diq.uhu.es; Fax: 0034 959 21 99 83; Tel: 0034 959 21 99 82

<sup>b</sup> Instituto de Tecnología Química, UPV-CSIC, Universidad Politécnica de Valencia, Av. de los Naranjos s/n, Valencia, E-46022, Spain

<sup>c</sup> Leibniz Institut für Katalyse e.V. an der Universität Rostock, Albert-Einstein-Str. 29a, D-18059 Rostock, Germany



**Scheme 1** Chemical structure of 1-(2-methoxynaphthalen-1-yl)-3-methyl-5,6,7,8-tetrahydroisoquinoline (**1**).

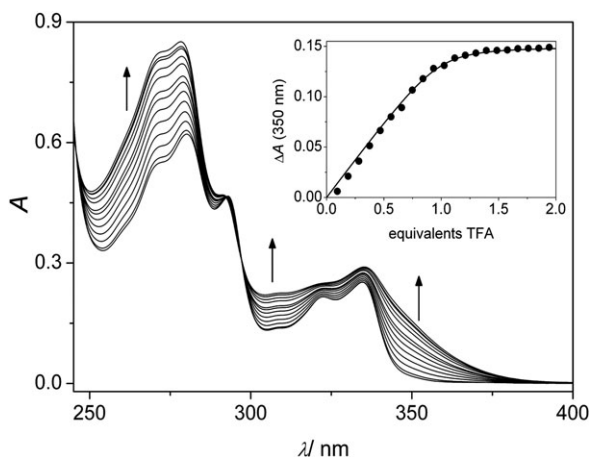


**Fig. 1** Absorption titration of **1** (76  $\mu\text{M}$ ) in acetonitrile. The shown spectra represent the titration range of 0–1.1 equivalents of TFA. The inset shows the titration curve at  $\lambda_{\text{obs}} = 350$  nm and the corresponding 1 : 1 fit.

states, resulting in the observed bathochromic absorption. Upon addition of trifluoroacetic acid (TFA) the spectrum changed dramatically, as a result of pyridine protonation (formation of  $1\text{H}^+$ ). Now a less structured and rather broad band, which extends to 400 nm (see Fig. 1), was observed. The fitting of the corresponding titration curve ( $\lambda_{\text{obs}} = 350$  nm) with a 1 : 1 model using HYPERQUAD 2003 yielded a protonation constant of  $\log K = 5.7$  (see inset of Fig. 1).<sup>22,23</sup> Several isosbestic points (246, 292 and 297 nm) have been observed in the course of the titration, typical for acid–base indicator equilibria. For the fluorescence measurements, which are described below, we have chosen 292 nm as reference excitation wavelength.<sup>‡</sup>

Unprotonated **1** displays a strong fluorescence (quantum yield  $\Phi_f = 0.26$ , lifetime  $\tau_f = 4.0$  ns, aerated acetonitrile) with a maximum at 353 nm. This behaviour is very similar to that obtained recently for a related naphthalene derivative without a pyridyl substituent [*N,N*-diethyl-2(*S*)-(6-methoxynaphth-2-yl)propionamide,<sup>24</sup>  $\Phi_f = 0.16$ ,  $\tau_f = 7.4$  ns, aerated acetonitrile; unpublished results]. This suggests the absence of quenching of the fluorescent naphthalene part by electron/charge or energy transfer involving the pyridyl residue. This assumption is in accordance with the unfavourable thermodynamics for these processes. Intramolecular energy transfer would be endergonic as the absorption spectrum of pyridine is

<sup>‡</sup> **1** is photostable under the applied experimental conditions. Irradiation for 5 h at  $\lambda_{\text{exc}} = 292$  nm with the Xe-lamp of the fluorimeter led to no significant changes in the fluorescence emission.

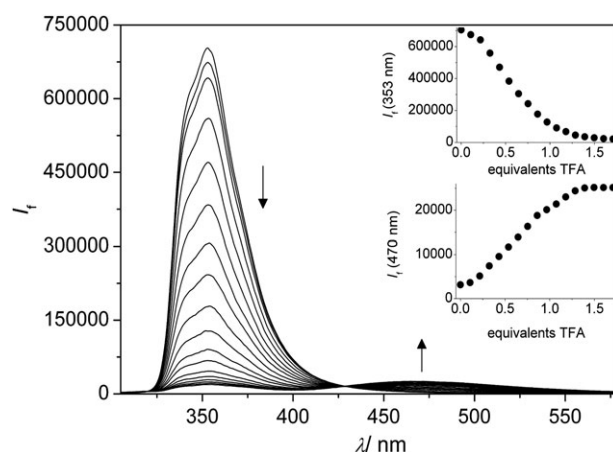


**Fig. 2** Changes in the fluorescence spectrum of **1** (29  $\mu\text{M}$  in acetonitrile) upon addition of TFA. The insets show the fluorescence intensities at  $\lambda_{\text{obs}} = 353$  nm (top) and 470 nm (bottom) in dependence on the amount of added TFA.

hypsochromically shifted with respect to that of 2-methoxynaphthalene and its derivatives. The thermodynamics for photoinduced electron (PET) or charge transfer (CT) can be estimated with the Rehm–Weller equation ( $\Delta G = E_{\text{ox}} - E_{\text{red}} - E^* + C$ ).<sup>25</sup> For the reduction ( $\Delta G = +1.00$  eV) as well as the oxidation ( $\Delta G = +0.42$  eV) of the naphthalene residue an endergonic thermodynamics results, using pyridine and 2-methoxynaphthalene as model compounds.<sup>26,27§</sup>

Akin to the observations made for the absorption spectrum, the addition of TFA changed the fluorescence spectrum drastically. The emission of the naphthalene chromophore is quenched and the concomitant growth of a broad band ( $\lambda_{f,\text{max}} = 470$  nm) with a smaller, but significant fluorescence quantum yield ( $\Phi_f = 0.04$ ) was observed, giving rise to an iso-emissive point (Fig. 2). The red-shifted emission is characteristic for an excited internal charge transfer (ICT) state, involving the methoxy-substituted naphthalene as donor and the protonated pyridine (*i.e.*, pyridinium ion) as acceptor.<sup>28</sup> The latter is a very strong electron acceptor (*cf.*  $E_{\text{red}} = -1.67$  V vs. SCE in acetonitrile for 2,4,6-trimethyl-*N*-methylpyridinium as model);<sup>29</sup> thus, an exergonic thermodynamics for intramolecular charge transfer results ( $\Delta G = -0.53$  eV).

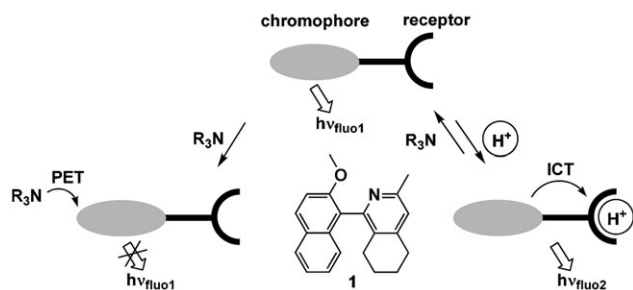
The excitation spectra monitoring the two emission channels (353 and 470 nm) coincide with the respective absorption spectra of **1** and  $1\text{H}^+$ , thereby confirming the authenticity of the observed fluorescence.

#### Fluorescence quenching of **1** by an electron-donating amine

The naphthalene fluorescence of **1** can be quenched by addition of *N,N*-diisopropyl-3-pentylamine (DiPPA), which acts as strong electron donor ( $E_{\text{ox}} = 0.72$  V vs. SCE in acetonitrile).<sup>30</sup>

§ The electrochemical oxidation ( $E_{\text{ox}}$ ) and reduction potentials ( $E_{\text{red}}$ ) of pyridine ( $E_{\text{ox}} = 2.12$  V; *cf.* ref. 27,  $E_{\text{red}} = -2.62$  V; *cf.* ref. 26) and 2-methoxynaphthalene ( $E_{\text{ox}} = 1.52$  V,  $E_{\text{red}} = -2.60$  V; *cf.* ref. 26) are stated for polar solvents (acetonitrile or *N,N*-dimethylformamide) and vs. the standard calomel reference electrode (SCE). The singlet excitation energy of **1** ( $E^* = 3.66$  eV) was derived from the intersection of the normalised absorption and fluorescence spectra. The Coulomb term *C* was taken as  $-0.06$  eV.





**Scheme 2** Switching between two fluorescent states involving **1** ( $h\nu_{\text{fluo1}} = 353 \text{ nm}$ ;  $h\nu_{\text{fluo2}} = 470 \text{ nm}$ ).  $\text{R}_3\text{N}$ : tertiary amine.

Based on preceding literature reports regarding the fluorescence quenching of naphthalenes by amines in polar solvents, we assume photoinduced electron transfer (PET) as effective quenching mechanism.<sup>31–33</sup> This process is thermodynamically allowed ( $\Delta G = -0.40 \text{ eV}$ ).

A plot of the fluorescence intensity of **1** at different DiPPA concentrations according to the Stern–Volmer equation ( $I_0/I = 1 + k_q\tau_0[\text{DiPPA}]$ ) yielded a straight line ( $n = 5$ ,  $r^2 = 0.998$ ). From the slope a bimolecular quenching rate constant of  $k_q = 1.8 \times 10^{10} \text{ M}^{-1} \text{ s}^{-1}$  was obtained, which corresponds to diffusion-controlled quenching in accordance with the exergonic PET thermodynamics.

### Boolean interpretation with an electron donor base (DiPPA) and trifluoroacetic acid (TFA) as inputs

The switching between the two fluorescence channels (output A: 353 nm, output B: 470 nm) by addition of acid defines TFA as one of the two chemical input species, which are required for the realisation of a logic operation. Furthermore, as discussed above, the fluorescence of **1** (output A) can be quenched by an electron-donating amine (DiPPA). However, DiPPA does not only act as electron donor, but also as strong organic base, which can neutralise TFA and thus leads to a reversible switching between the fluorescence signals caused by **1** and the ICT state observed for  $\text{1H}^+$ . These pathways are generalised in Scheme 2, suggesting that this principle might be applied not only for **1**, but for a variety of fluorophore–receptor combinations.

The input-dependent fluorescence spectra of **1** are shown in Fig. 3 (top). The naphthalene fluorescence at 353 nm (output A) is strongest in the absence and simultaneous presence of both inputs.<sup>¶</sup> On the other hand, protonation or PET-induced amine quenching leads to a smaller output signal. By defining negative logic for this output channel (binary encoding: low signal = 1, high signal = 0), the truth table of an *XOR* gate is obtained (Table 1). *XOR* gates are of high value for combinatorial logic circuits, which are capable of arithmetic number processing.<sup>5</sup> In combination with an *AND* gate a half-adder is

<sup>¶</sup> In the simultaneous presence of both inputs, the signal was somewhat lower than without inputs. However, one should recall that the effective acid concentration, which is needed to quench 80% of the naphthalene fluorescence via formation of a CT state is ca. 600 times lower as compared to the necessary DiPPA concentration for the logic gate simulation. Thus, small deviations from neutrality (within experimental error) could have already an important impact on the complete recovery of the fluorescence signal in the presence of both inputs.

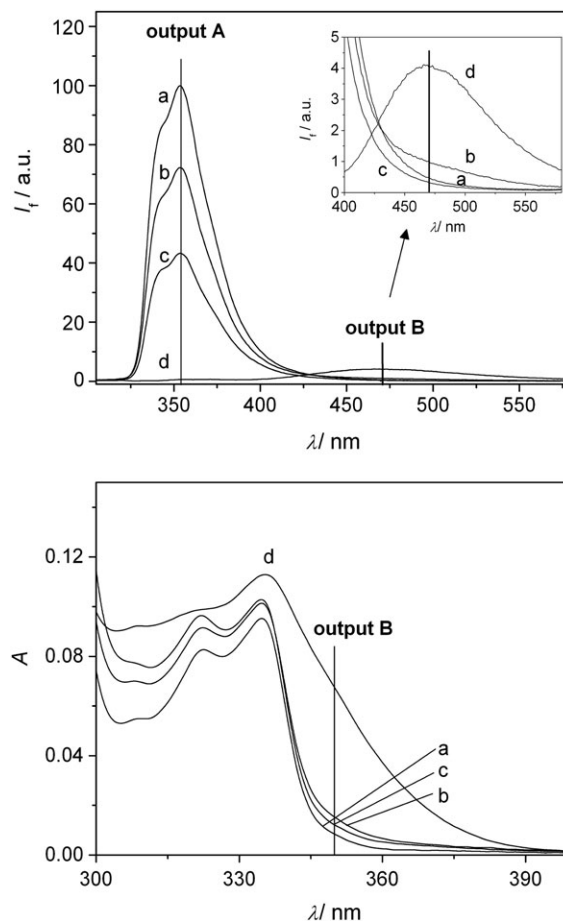


**Fig. 3** Input-dependent changes of the fluorescence (top) and absorption (bottom) spectra of **1**: (a) only **1**, (b) **1** + TFA + DiPPA, (c) **1** + DiPPA, (d) **1** + TFA (for concentrations see footnotes *d* and *e* of Table 1).

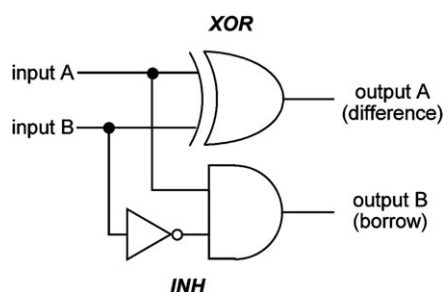
obtained, while logic circuits composed of *XOR* and *INH* (inhibit) gates integrate the function of a half-subtractor.

In our system the second fluorescence output at 470 nm (output B) corresponds to an *INH* gate (positive logic con-

**Table 1** Truth table for the logic behaviour of **1** (29  $\mu\text{M}$  in acetonitrile) with TFA and DiPPA as inputs

Input A TFA <sup>d</sup>	Input B DiPPA <sup>e</sup>	Output A <sup>a,b</sup> ( <i>XOR</i> ) $\lambda_f = 353 \text{ nm}$	Output B <sup>a,c</sup> ( <i>INH</i> )	
			$\lambda_f = 470 \text{ nm}$	$\lambda_{\text{abs}} = 350 \text{ nm}$
0	0	0 (100)	0 (12)	0 (0.008)
0	1	1 (43) <sup>f</sup>	0 (8)	0 (0.012)
1	0	1 (1)	1 (100)	1 (0.067)
1	1	0 (72)	0 (25)	0 (0.015)

<sup>a</sup> In parentheses, the relative fluorescence intensity for each channel or absorbance *A* (last column) is given. For each output channel a threshold of 50% of the respective highest signal was applied. <sup>b</sup> Application of negative logic convention. Application of a positive logic convention leads to opposite output binary values in column 3, which corresponds to an *XNOR* gate. <sup>c</sup> Application of positive logic convention. <sup>d</sup> [TFA] = 17.5 mM. <sup>e</sup> [DiPPA] = 17.5 mM for fluorescence and 19.7 mM for absorption. <sup>f</sup> The threshold could still be lowered by applying a higher amine concentration, e.g., 40 mM DiPPA would lead to a smaller residual signal (26 vs. 43% for 17.5 mM DiPPA).

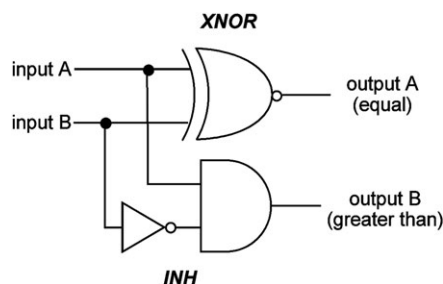


**Scheme 3** Symbolisation of a half-subtractor.

vention for the output; high = 1, low = 0), which can be interpreted as an *AND* gate with one of the inputs being inverted. The strongest signal for this channel, based on the discussed ICT state, is observed in the sole presence of TFA. All other input combinations do not contribute to the formation of that state or lead to its destruction *via* acid–base-neutralisation (input A = input B = 1). These observations are summarised in Table 1. Alternatively, the same logic operation can be obtained by monitoring the changes in the absorption spectrum at  $\lambda_{\text{obs}} = 350$  nm (see Fig. 3, bottom). Noteworthy, the definition of a different logic convention for each fluorescence output channel, *i.e.*, 353 and 470 nm, is totally legitimate, because the gates are operated individually.<sup>13</sup>

As mentioned above, the combination of both logic gates yields a half-subtractor, with the *XOR* output as difference and the *INH* output as borrow (see Scheme 3).<sup>11–17,19,20</sup> The result of the subtraction “input B – input A” corresponds to the difference (output A), thereby yielding 0 – 0 = 0, 1 – 0 = 1, and 1 – 1 = 0. In the case “input B < input A” a “1” is borrowed (output B) from the next higher stage, which leads to 2 – 1 = 1.

Applying a positive logic convention for both output channels yields a *XNOR/INH* combination as shown in Scheme 4. This particular logic circuit works as a magnitude comparator.<sup>18</sup> If both inputs are equal, the output of the *XNOR* gate (output A, corresponding to the 353 nm fluorescence signal) is 1. This is the case for the simultaneous presence or absence of the inputs (input A = input B = 0 or 1). For the case that the inputs are not of equal binary magnitude, the value of the *XNOR* output is 0. The superposed *INH* function (470 nm fluorescence channel) helps to decide if input A > input B or input A < input B applies: the output is 1 if input A is greater than input B and 0 for the opposite situation. Thus, the three possible situations input A = input B, input A > input B, and input A < input B are clearly distinguished by distinct



**Scheme 4** Symbolisation of a magnitude comparator.

*XNOR/INH* output combinations, *i.e.*, 1/0, 0/1, 0/0, respectively (see Table 1 and footnote *b* in that table).

In the context of using inputs, which interact intermolecularly (*e.g.*, the amine DiPPA) with a gate, it is interesting to note that many molecular logic systems use intuitively different receptor units for the recognition of chemical inputs. A commonly encountered example for input-dependent receptor–fluorophore communication is based on covalently-linked PET-active amino functions, which can be blocked by protonation or metal coordination.<sup>34</sup> However, the recognition of a chemical input by a receptor is not a precondition for the operation of a molecular logic system, as has been demonstrated for example for oxygen as input.<sup>35–39</sup> Thus, the design of molecular logic systems could be simplified by applying *intermolecular* PET. However, it should be mentioned here, that due to the unspecific nature of the interaction, a strict chemical definition of an unimolecular system is desirable. Otherwise, input-sided cross talk between chemically distinguished logic gates might potentially lead to complications.

### Boolean interpretation with $\text{H}_2\text{PO}_4^-$ and TFA as inputs

The substitution of the electron-donating amine DiPPA by the PET-inactive dihydrogenphosphate anion ( $\text{H}_2\text{PO}_4^-$ , tetrabutylammonium salt), while keeping TFA as input A, results in a reconfiguration of the logic behaviour of **1**. Pyridinium moieties can interact with dihydrogenphosphate anions by electrostatic interactions and hydrogen bonding involving the  $\text{NH}^+$ ,<sup>40</sup> which we presume to apply also to  $1\text{H}^+$ . Expectedly, this led to similar effects (switching from ICT fluorescence at 470 nm to naphthalene fluorescence at 353 nm) as observed upon addition of DiPPA. Consequently, the fluorescence behaviour of the 470 nm output is again compatible with *INH* logic (Fig. 4 and Table 2). The same applies to the changes in the absorption spectrum (spectra very similar to Fig. 3, bottom). However, the situation is different for the naphthalene fluorescence at 353 nm (output A). Contrary to DiPPA,  $\text{H}_2\text{PO}_4^-$  anions are not involved in PET-induced fluorescence quenching of **1**. Thus, an implication (*IMP*) gate,<sup>41</sup> which is output-complementary to an *INH* gate, is

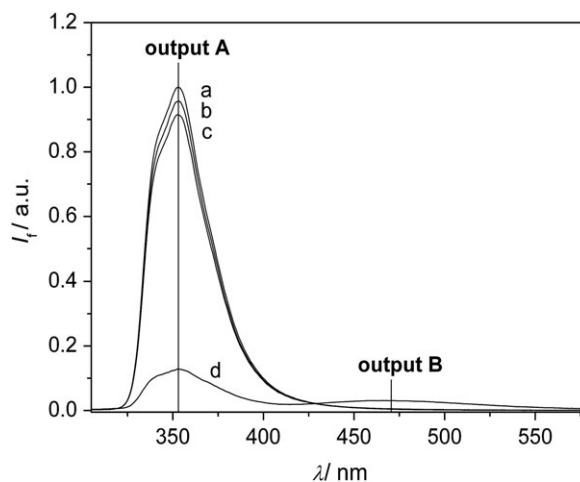


**Fig. 4** Input-dependent changes of the fluorescence spectrum of **1** (29  $\mu\text{M}$  in acetonitrile): (a) only **1**, (b) **1** +  $\text{H}_2\text{PO}_4^-$  (46  $\mu\text{M}$ ), (c) **1** + TFA (31  $\mu\text{M}$ ) +  $\text{H}_2\text{PO}_4^-$  (46  $\mu\text{M}$ ), (d) **1** + TFA (31  $\mu\text{M}$ ).

**Table 2** Truth table for the logic behaviour of **1** (29  $\mu\text{M}$  in acetonitrile) with TFA and  $\text{H}_2\text{PO}_4^-$  anions as inputs

Input A TFA	Input B $\text{H}_2\text{PO}_4^-$	Output A <sup>a</sup> (IMP) $\lambda_f = 353 \text{ nm}^b$	Output B <sup>a</sup> (INH)	
			$\lambda_f = 470 \text{ nm}^b$	$\lambda_{\text{abs}} = 350 \text{ nm}^c$
0	0	1 (100)	0 (15)	0 (0.008)
0	1	1 (96)	0 (15)	0 (0.008)
1	0	0 (13)	1 (100)	1 (0.055)
1	1	1 (91)	0 (18)	0 (0.013)

<sup>a</sup> In parentheses, the relative fluorescence intensity for each channel or absorbance  $A$  (last column) is given. For each output channel a threshold of 25% of the respective highest signal was applied; positive logic convention. <sup>b</sup> [TFA] = 31  $\mu\text{M}$ , [ $\text{H}_2\text{PO}_4^-$ ] = 46  $\mu\text{M}$ . <sup>c</sup> [TFA] = 30  $\mu\text{M}$ , [ $\text{H}_2\text{PO}_4^-$ ] = 45  $\mu\text{M}$ .

obtained. In Table 2 the corresponding chemical inputs, fluorescence output signals, and their binary encoding are compiled. Implication logic is closely related to “if... (condition), then... (consequence)” phrases. In the context of logic interpretation these statements are always true (output A = 1), except a true condition (input A = 1) implies a false consequence (input B = 0).

Finally, both logic gates can be combined in a complementary output circuit, whose electronic equivalent is shown in Scheme 5. Notably, Shanzer and co-workers reported recently another example for an output-complementary logic circuit, which integrates parallel working YES and NOT gates.<sup>42</sup> In electronics, complementary outputs are commonly generated by operating two identical logic gates in parallel and inverting the output of one of them with a NOT gate.<sup>43</sup> However, this leads to an unwanted time lag for the inverted output. On the other hand, the superposition of optical molecular logic gates, as in the present case, enables the simultaneous read out of both fluorescence outputs without any time delay.

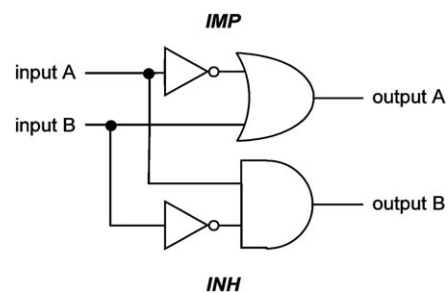
## Conclusions

In summary, we have demonstrated the unimolecular implementation of various logic gates (XOR, XNOR, INH, IMP), which can be reconfigured either by input variations or intelligent selection of optical output channels. Combinations of the particular gates yield advanced and so far scarcely reported molecular logic devices, namely a half-subtractor, a magnitude comparator, and a complementary output circuit. We contend that the combination of such general concepts such as intermolecular PET-induced fluorescence quenching and ICT fluorescence emission, which constitute the basis for the herein discussed implementation of logic operations, will lead to further examples of reconfigurable unimolecular devices with advanced logic capabilities.

## Experimental

### Materials

All commercial chemicals (*N,N*-diisopropyl-3-pentylamine, trifluoroacetic acid, naphthalene, tetrabutylammonium dihydrogenphosphate) were of highest purity available ( $\geq 99\%$ ) and used as received. Solvents (acetonitrile, ethanol) were of

**Scheme 5** Symbolisation of a complementary output IMP/INH circuit.

HPLC quality. The synthesis of compound **1** via a photo-induced Co(i)-catalysed [2 + 2 + 2] cycloaddition between 2-methoxy-1-(1,7-octadiynyl)naphthalene and acetonitrile and its characterisation have been reported recently.<sup>44</sup>

### Photophysical measurements

Absorption measurements were done with a Perkin Elmer Lambda 35 UV/Vis spectrometer. Steady-state fluorescence measurements were carried out on a Photon Technology International (PTI) LPS-220B spectrofluorimeter. The fluorescence lifetime measurement was done on a setup from Edinburgh Instruments (nF 920) with a nanosecond hydrogen flashlamp (1.5 ns pulse width) and by applying deconvolution from the lamp pulse. Titration experiments were performed by administering aliquots of a stock solution of the titrant to a quartz cuvette with 3.5 ml of the titrand solution. In order to minimise concentration changes in the course of the titration maximal 70  $\mu\text{l}$  stock solution were added. All experiments were done at room temperature (23  $^{\circ}\text{C}$ ) and in aerated solution. The fluorescence quantum yields were measured for  $\lambda_{\text{exc}} = 292 \text{ nm}$  with naphthalene as standard ( $\Phi_f = 0.21$ , degassed ethanol).<sup>45</sup>

## Acknowledgements

The financial support by the Spanish Ministry of Education and Science, Madrid (Ramón y Cajal grant for U. P.), the Instituto de Tecnología Química (Valencia), and the Universidad de Huelva is gratefully acknowledged. The measurement of the fluorescence lifetime of **1** was done by Dr H. Sahoo (Jacobs University Bremen, Germany).

## References

- F. M. Raymo, *Adv. Mater.*, 2002, **14**, 401–414.
- V. Balzani, A. Credi and M. Venturi, *ChemPhysChem*, 2003, **4**, 49–59.
- A. P. de Silva and N. D. McClenaghan, *Chem.–Eur. J.*, 2004, **10**, 574–586.
- A. P. de Silva, Y. Leydet, C. Lincheneau and N. D. McClenaghan, *J. Phys.: Condens. Matter*, 2006, **18**, S1847–S1872.
- U. Pischel, *Angew. Chem., Int. Ed.*, 2007, **46**, 4026–4040.
- A. P. de Silva, S. S. K. de Silva, N. C. W. Goonesekera, H. Q. N. Gunaratne, P. L. M. Lynch, K. R. Nesbitt, S. T. Patuwathavithana and N. L. D. S. Ramyalal, *J. Am. Chem. Soc.*, 2007, **129**, 3050–3051.
- J. Andréasson, G. Kodis, Y. Terazono, P. A. Liddell, S. Bandyopadhyay, R. H. Mitchell, T. A. Moore, A. L. Moore and D. Gust, *J. Am. Chem. Soc.*, 2004, **126**, 15926–15927.

- 8 A. P. de Silva and N. D. McClenaghan, *J. Am. Chem. Soc.*, 2000, **122**, 3965–3966.
- 9 H. T. Baytekin and E. U. Akkaya, *Org. Lett.*, 2000, **2**, 1725–1727.
- 10 A. P. de Silva and N. D. McClenaghan, *Chem.-Eur. J.*, 2002, **8**, 4935–4945.
- 11 S. J. Langford and T. Yann, *J. Am. Chem. Soc.*, 2003, **125**, 11198–11199.
- 12 D. Margulies, G. Melman, C. E. Felder, R. Arad-Yellin and A. Shanzer, *J. Am. Chem. Soc.*, 2004, **126**, 15400–15401.
- 13 A. Coskun, E. Deniz and E. U. Akkaya, *Org. Lett.*, 2005, **7**, 5187–5189.
- 14 F. Li, M. Shi, C. Huang and L. Jin, *J. Mater. Chem.*, 2005, **15**, 3015–3020.
- 15 D. Margulies, G. Melman and A. Shanzer, *Nat. Mater.*, 2005, **4**, 768–771.
- 16 D. Margulies, G. Melman and A. Shanzer, *J. Am. Chem. Soc.*, 2006, **128**, 4865–4871.
- 17 R. Baron, O. Lioubashevski, E. Katz, T. Niazov and I. Willner, *Angew. Chem., Int. Ed.*, 2006, **45**, 1572–1576.
- 18 Y. Liu, W. Jiang, H.-Y. Zhang and C.-J. Li, *J. Phys. Chem. B*, 2006, **110**, 14231–14235.
- 19 M. Suresh, D. A. Jose and A. Das, *Org. Lett.*, 2007, **9**, 441–444.
- 20 E. Pérez-Inestrosa, J.-M. Montenegro, D. Collado, R. Suau and J. Casado, *J. Phys. Chem. C*, 2007, **111**, 6904–6909.
- 21 L. J. Martinez and J. C. Scaiano, *Photochem. Photobiol.*, 1998, **68**, 646–651.
- 22 P. Gans, A. Sabatini and A. Vacca, *Talanta*, 1996, **43**, 1739–1753.
- 23 L. Alderighi, P. Gans, A. Ienco, D. Peters, A. Sabatini and A. Vacca, *Coord. Chem. Rev.*, 1999, **184**, 311–318.
- 24 S. Abad, U. Pischel and M. A. Miranda, *J. Phys. Chem. A*, 2005, **109**, 2711–2717.
- 25 D. Rehm and A. Weller, *Ber. Bunsenges. Phys. Chem.*, 1969, **73**, 834–839.
- 26 M. Montalti, A. Credi, L. Prodi and M. T. Gandolfi, *Handbook of Photochemistry*, CRC Press Taylor & Francis, Boca Raton FL, 3rd edn, 2006.
- 27 P. Jacques, D. Burget, X. Allonas and J. P. Fouassier, *Chem. Phys. Lett.*, 1994, **227**, 26–32.
- 28 N. B. Sankaran, S. Banthia, A. Das and A. Samanta, *New J. Chem.*, 2002, **26**, 1529–1531.
- 29 H.-Y. Chao, W. Lu, Y. Li, M. C. W. Chan, C.-M. Che, K.-K. Cheung and N. Zhu, *J. Am. Chem. Soc.*, 2002, **124**, 14696–14706.
- 30 U. Pischel, X. Zhang, B. Hellrung, E. Haselbach, P.-A. Muller and W. M. Nau, *J. Am. Chem. Soc.*, 2000, **122**, 2027–2034.
- 31 F. Meeus, M. Van der Auweraer and F. C. De Schryver, *J. Am. Chem. Soc.*, 1980, **102**, 4017–4024.
- 32 T. Yoroazu, K. Hayashi and M. Irie, *J. Am. Chem. Soc.*, 1981, **103**, 5480–5484.
- 33 U. Pischel, S. Abad and M. A. Miranda, *Chem. Commun.*, 2003, 1088–1089.
- 34 A. P. de Silva, H. Q. N. Gunaratne, T. Gunnlaugsson, A. J. M. Huxley, C. P. McCoy, J. T. Rademacher and T. E. Rice, *Chem. Rev.*, 1997, **97**, 1515–1566.
- 35 D. Parker and J. A. G. Williams, *Chem. Commun.*, 1998, 245–246.
- 36 A. P. de Silva, I. M. Dixon, H. Q. N. Gunaratne, T. Gunnlaugsson, P. R. S. Maxwell and T. E. Rice, *J. Am. Chem. Soc.*, 1999, **121**, 1393–1394.
- 37 T. Gunnlaugsson, D. A. Mac Dónaill and D. Parker, *J. Am. Chem. Soc.*, 2001, **123**, 12866–12876.
- 38 M. de Sousa, M. Kluciar, S. Abad, M. A. Miranda, B. de Castro and U. Pischel, *Photochem. Photobiol. Sci.*, 2004, **3**, 639–642.
- 39 M. de Sousa, B. de Castro, S. Abad, M. A. Miranda and U. Pischel, *Chem. Commun.*, 2006, 2051–2053.
- 40 P. E. Kruger, P. R. Mackie and M. Nieuwenhuyzen, *J. Chem. Soc., Perkin Trans. 2*, 2001, 1079–1083.
- 41 M. Sarkar, S. Banthia, A. Patil, M. B. Ansari and A. Samanta, *New J. Chem.*, 2006, **30**, 1557–1560.
- 42 D. Margulies, C. E. Felder, G. Melman and A. Shanzer, *J. Am. Chem. Soc.*, 2007, **129**, 347–354.
- 43 T. R. Kuphaldt, *Lessons in Electric Circuits, Volume IV - Digital* available under [www.ibiblio.org/obp/electricCircuits](http://www.ibiblio.org/obp/electricCircuits) (Open Book Project), 4th edn, 2006.
- 44 A. Gutnov, B. Heller, C. Fischer, H.-J. Drexler, A. Spannenberg, B. Sundermann and C. Sundermann, *Angew. Chem., Int. Ed.*, 2004, **43**, 3795–3797.
- 45 C. A. Parker and T. A. Joyce, *Trans. Faraday Soc.*, 1966, **62**, 2785–2792.